High-Resolution Structure and Conformational Dynamics of Rigid, Cofacially Aligned Porphyrin−Bridge−Quinone Systems As Determined by NMR Spectroscopy and ab Initio Simulated Annealing Calculations

Peter M. Iovine,[†] Gianluigi Veglia,[‡] George Furst,[†] and Michael J. Therien*,[†]

Contribution from the Department of Chemistry, University of Pennsylvania, Philadelphia, Pennsylvania 19104-6323, and Department of Chemistry, University of Minnesota, Minneapolis, Minnesota 55455

Received January 2, 2001

Abstract: The high-resolution solution structure and dynamics of a cofacially aligned porphyrin−phenylene−quinone compound have been determined using ^{1}H NMR spectroscopy and simulated annealing calculations. Members of this class of π-stacked assemblies feature a 1,8-naphthyl pillaring motif that enforces sub van der Waals interplanar separations between juxtaposed porphyryl, aromatic bridge, and quinonyl components of the donor−spacer−acceptor compound; this structural motif gives rise to a comprehensive set of structurally significant NOE signatures that can be used as constraints in quantitative structural calculations. Examination of such data using ab initio simulated annealing analytical methods shows that 5-[8′-(4″-[8‴-(2⁗,5‴-benzoquinonyl)-1‴-naphthyl]-1″-phenyl)-1′-naphthyl]-10,20-diphenylporphyrin displays an unusual degree of conformational homogeneity in the condensed phase, and represents a rare example where such an analysis determines unequivocally a single unique structure in solution.

Introduction

Analysis of structure-dependent spectroscopic properties in the condensed phase requires knowledge of the nature of the dynamical motions available to the compound of interest. With such information, key structure−function and structure−property relationships can be ascertained independent of the assumption that the liquid-phase structure is identical to that determined for the solid state by X-ray crystallographic methods.

We have recently reported the synthesis of a new series of rigid, π-stacked, porphyrin−bridge−quinone systems that differ in many respects from other classes of donor−spacer−acceptor (D-Sp-A) systems that feature cofacial aromatic residues separating D from A.[1] In these systems, a 1,8-naphthyl pillaring motif enforces sub van der Waals interplanar separations between juxtaposed porphyryl, aromatic bridge, and quinonyl components of the D-Sp-A compound. The compact nature of these assemblies limits severely the range of allowable nuclear dynamical motions, maintaining constant distance and lateral shift between the adjacent D, Sp, and A units in the π-stacked array.

These highly compact, stacked multiaromatic structures manifest a number of unusual features in their NMR spectra. For example, 5-[8′-(4″-[8‴-(2⁗,5‴-benzoquinonyl)-1‴-naphthyl]-1″-phenyl)-1′-naphthyl]-10,20-diphenylporphyrin (**1**), a member of this class of structures, evinces ^{1}H nuclei constrained to reside in unusual and diverse magnetic environments: the 38 aromatic proton resonances of this species are extraordinarily well resolved, and are distributed uniformly over a 10.20-to-0.62 ppm spectral window.[1] These spectral features combined with the extensive *J*-coupling network enabled the unambiguous assignment of all the resonances using conventional COSY and NOESY 2-D NMR experiments.

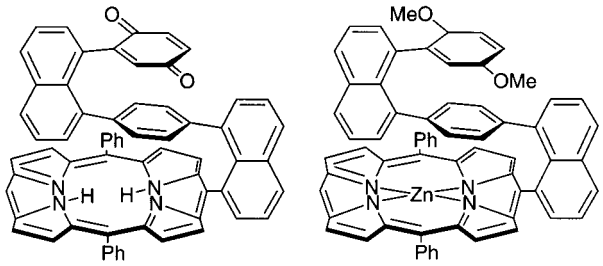

1 **2**

2-D Nuclear Overhauser Effect NMR spectroscopy (NOESY) experiments carried out in tandem with ab initio simulated annealing (SA) calculations[2−6] represent a powerful approach to probe solution structure. Because of **1**'s limited conformational mobility, such methods offer the potential to determine condensed-phase structural parameters. Similar approaches have been used by Baringhaus to probe the solution structure of a dialkylboron enolate[10] and by Bruice to assess the ground-state

[†] University of Pennsylvania.
[‡] University of Minnesota.

(1) Iovine, P. M.; Kellett, M. A.; Redmore, N. P.; Therien, M. J. *J. Am. Chem. Soc.* **2000**, *122*, 8717−8727.
(2) Nilges, M.; Clore, G. M.; Gronenborn, A. M. *FEBS Lett.* **1988**, *239*, 129−136.
(3) Kirkpatrick, S.; Gelatt, C. C., Jr.; Vecchi, M. P. *Science* **1983**, *220*, 671.
(4) Wilson, S. R.; Cui, W. *Biopolymers* **1990**, *29*, 225.
(5) Wilson, S. R.; Cui, W.; Moskowitz, J. W.; Schmidt, K. E. *J. Comput. Chem.* **1991**, *12*, 342.
(6) Okamoto, Y.; Kikuchi, T.; Kawai, H. *Chem. Lett.* **1992**, *3*, 1275.
(7) Brünger, A. T.; Clore, G. M.; Gronenborn, A. M.; Karplus, M. *Proc. Natl. Acad. Sci. U.S.A.* **1986**, *83*, 3801.

10.1021/ja010023t CCC: $20.00
Published on Web 05/22/2001

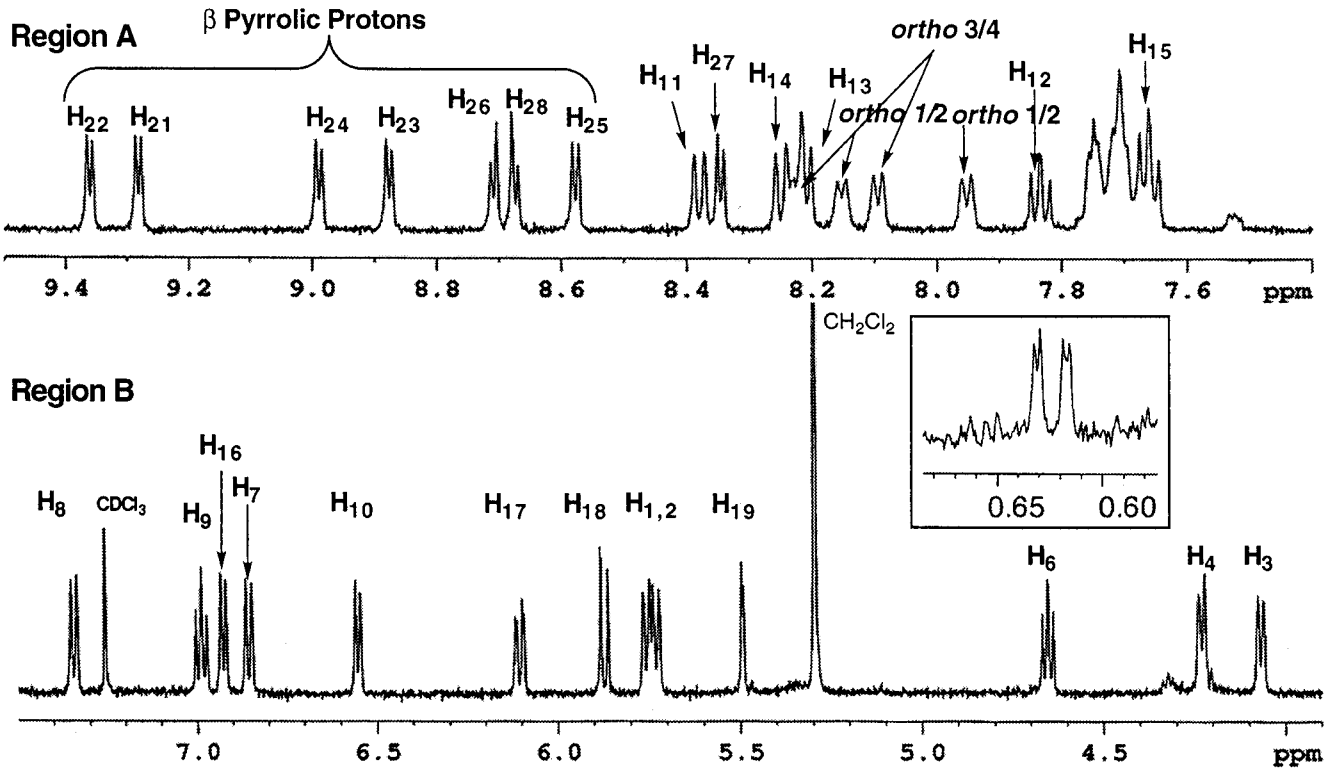

Figure 1. 500 MHz ^{1}H NMR spectrum of 5-[8′-(4″-[8‴-(2⁗,5⁗-benzoquinonyl)-1‴-naphthyl]-1″-phenyl)-1′-naphthyl]-10,20-diphenylporphyrin (**1**) in $CDCl_3$. Spectral regions A and B are shown as expansions of the full spectrum.

structures of several facially capped porphyrin compounds based on the cyclophane motif.[11,12] The favorable structural and spectroscopic properties of these newly defined π-stacked D-Sp-A assemblies allowed the acquisition of a substantial number of structurally significant NOEs which define key interplanar relationships between the porphyrin, phenyl spacer, and benzoquinonyl units; these data were incorporated as restraining functions in the ab initio simulated annealing calculations, enabling a high-resolution solution structure of **1** to be determined.

Experimental Section

NMR Spectroscopy. NMR spectra were recorded on a 500-MHz AMX Bruker spectrometer. Sample concentrations were typically 14 mM in $CDCl_3$ (Cambridge Isotope Laboratories). All samples were degassed via 3 freeze−pump−thaw cycles. The chemical shifts for ^{1}H NMR spectra were referenced to internal TMS (δ = 0.00 ppm). Resonance assignments in compound **1** were based on analyses of 1-D ^{1}H NMR spectral data and the DQF-COSY spectrum (2 K points in the acquisition dimension and 512 points in the indirect dimension) reported herein for [5-(8′-[4″-(8‴-[2⁗, 5⁗-dimethoxyphenyl]-1‴-naphthyl)-1″-phenyl]-10,20-diphenylporphinato]zinc(II).[1]

2D NOESY. Two-dimensional phase-sensitive NOESY spectra[13] were taken at different mixing times (50, 100, 200, 400, 600, 800, 1000 and 1200 ms) to ensure the linearity of the NOE volume buildup with respect to the mixing time τ_m. The NOESY spectrum obtained at τ_m = 800 ms was chosen for quantitating NOESY volume integrals due to the lack of spin diffusion. The data were processed on a Silicon Graphics O_2 workstation using the software program XWINMR. Spectral data were obtained in 1 K complex points in the acquisition dimension and 512 points in the indirect dimension. The data were zero-filled to double the size, and apodized with a sine squared window function in both dimensions. The volumes of the NOE cross-peaks were integrated using the routine built in the program Felix 98 integrated with Insight II (Molecular Simulations Inc., San Diego, CA). The interproton distances were calculated using the equation

$$r_a = r_b(\mathrm{NOE}_b/\mathrm{NOE}_a)^{1/6} \quad (1)$$

where r_a is the proton−proton distance of interest, r_b is a known proton−proton distance (i.e. H_7-H_8, 2.374 Å Figure 2), and NOE_a and NOE_b are the cross-peak volume integrals extracted from the NOESY spectra. For these studies, the calibration distance, r_b, corresponds to the X-ray crystallographically determined separation between the H_4 and H_5 atoms of 1,8-diphenylnaphthalene.[14−16]

NMR Structure Calculations. The absence of an X-PLOR force field for compound **1** necessitated the development of a reliable parameter set that would be employed in all subsequent X-PLOR NMR structural calculations. The complete force field (parameter and topology files) is contained in the Supporting Information. The compound **1** force field was developed using the porphyryl residue topology file (porphyrin.rtf) supplied with the Quanta software package (Molecular Simulations Inc., San Diego, CA) while the ChemNote facility of Quanta was used to construct the naphthalene pillar, phenyl spacer, and quinone acceptor moieties and the corresponding linkages between these components. The composite structure was then exported in PDB format for use in X-PLOR (Molecular Simulations Inc., San Diego, CA, Version 3.81). The molecular coordinates from this initial structure

(8) Kuszewski, J.; Nilges, M.; Brünger, A. T. *J. Biomol. NMR* **1992**, *2*, 33−56.
(9) Powers, R.; Garrett, D. S.; March, C. J.; Frieden, E. A.; Gronenborn, A. M.; Clore, G. M. *Biochemistry* **1993**, *32*, 2.
(10) Baringhaus, K.-H.; Matter, H.; Kurz, M. *J. Org. Chem.* **2000**, *65*, 5031−5033.
(11) Zhang, H. Y.; Blasko, A.; Yu, J. Q.; Bruice, T. C. *J. Am. Chem. Soc.* **1992**, *114*, 6621−6630.
(12) Blasko, A.; Barbara, G.; Bruice, T. C. *J. Org. Chem.* **1993**, *58*, 5738−5747.
(13) Jeener, J.; Meier, B. H.; Bachman, P.; Ernst, R. R. *J. Chem. Phys.* **1979**, *71*, 4546.
(14) House, H. O.; Koepsell, D. G.; Campbell, W. J. *J. Org. Chem.* **1972**, *37*, 1003−1011.
(15) Clough, R. L.; Kung, W. J.; Marsh, R. E.; Roberts, J. D. *J. Org. Chem.* **1976**, *41*, 3603−3609.
(16) Tsuji, R.; Kamatsu, K.; Takeuchi, K.; Shiro, M.; Cohen, S.; Rabinovitz, M. *J. Phys. Org. Chem.* **1993**, *6*, 435−444.

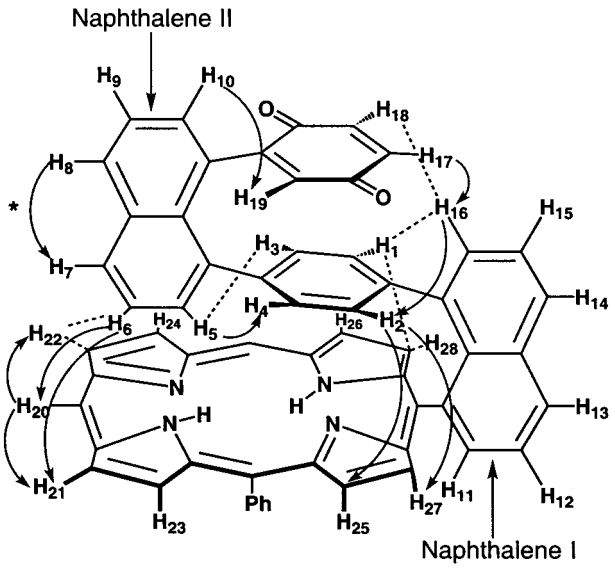

Figure 2. Proton labeling schematic for compound **1**. Compound **1**'s observed NOESY signals are highlighted using curved arrow notation. The NOE marked with an asterisk was utilized as a known separation distance (2.374 Å).[14,15]

were used to generate a molecular template coordinate set[17] with arbitrary extended conformation. The simulated annealing protocol is based on an MD simulation with subsequent cooling steps to drive the system toward its low-energy state.[3−6,18]

The target bond and angle parameters for the porphyrin moiety were extracted from the X-ray crystallographic data of 5-(2′,5′,2″,5″-tetrafluoro-2‴,5‴dimethoxy[1′,1″,4″,1‴]terphenyl-4′-yl)-10,20-diphenylporphyrin.[19] Dihedral angle parameters for the porphyrin macrocycle were set to either 0 or 180° depending on their cisoid or transoid configuration in an ideal planar macrocycle. Improper torsional angles of the porphyrin were fixed to maintain planarity. The naphthyl and spacer-phenyl bond, angle, and dihedral angle parameters were based on X-ray crystallographic data obtained by House[14−16] for 1,8-diphenylnaphthalene; the quinonyl moiety was parametrized using X-ray crystallographic data published by Rees.[20] All force constants used in the X-PLOR-based NMR structural determination were the program default values (bonds, 1000 kcal mol^{-1} $Å^{-2}$; dihedral angles, 750 kcal mol^{-1}; improper angles, 750 kcal mol^{-1}; and other angles, 500 kcal mol^{-1} rad^{-2}) required to maintain the covalent geometry during the high-temperature molecular dynamics steps. Standard masses were taken for C, H, N, and O in the structure file.

Ab Initio Simulated Annealing. Starting from an extended structure of compound **1**, 50 different conformers were generated using the standard ab initio simulated annealing protocols[2,17] with the NOE values summarized in Table 1 as a restraint file. The lower bounds of the proton−proton constraints were set to the sum of the van der Waals radii while the upper bound was set to 10% higher than the calculated distances.[11,12] An initial minimization (Powell, 50 steps) was performed followed by the high-temperature molecular dynamics. For an efficient conformational sampling, 6000 steps of molecular dynamics were performed at 2000 K with a time step of 0.005 ps. The total number of cooling steps was 1000 to reach a final temperature of 100 K. A final stage of 200 steps of Powell minimization was used to minimize the 50 structures generated. The 50 structures generated from the ab initio simulated annealing were further refined using the *refine-gentle* procedure as described by Brünger,[17] which employs the full Lennard-Jones potential and thus includes repulsive and attractive terms as well as electrostatic factors in the calculation of the nonbonded energies. The initial temperature for this final refinement was 300 K. The simulated annealing time step was 0.0001 ps as to allow a gradual introduction of the full van der Waals radii for the nuclei. As a computational control experiment, ab initio simulated annealing calculations of compound **1** in the absence of NOESY-derived distance restraints were performed to determine the effect of the constraints on the conformational search. The unrestrained calculations utilized the identical parameter set (Supporting Information) as was employed in the X-Plor MD/SA calculation with constraints. In addition, all user inputted variables in the ab initio simulated annealing calculations remained unchanged with respect to those used in the calculations with distance constraints, including those relevant to the slow cooling refinement process.

Final CHARMm Restrained Minimizations of ab Initio Simulated Annealing Derived Structures. The 50 structures generated were minimized using the CHARMm force field[21] with the 11 NOESY-derived constraints to obtain final CHARMm energies. The CHARMm constraint potential function[21] parameters RMIN and RMAX were maintained at identical values as were used in the XPLOR NMR structural determination calculations (RMIN = proton−proton van der Waals contact distance (1.90 Å); RMAX = 1.10 times the proton−proton distance determined from the NOESY spectral data). The force constant parameters KMIN and KMAX[21] were set to 15 kcal/(mol·$Å^2$) and describe the steepness of the NOE constraint potential function outside of the user-defined potential width. Increasing or decreasing the KMIN and KMAX parameters by up to 10 kcal/(mol·$Å^2$) did not significantly affect the final energy or the resultant structure. The CHARMm force field parameters for compound **1** are tabulated in the Supporting Information. Minimizations were performed for approximately 6000 steps or until the energy difference between successive minimizations was less than 1×10^{-9} kcal/mol. The nonbonded lists, which describe through-space proton−proton contact distances, were updated every 5 steps; a standard nonbonded cutoff distance of 14.5 Å was used in these calculations.

Results and Discussion

1- and 2-D Spectral Assignments and Characteristics. Complete and unambiguous assignment of the ^{1}H NMR resonances for **1** was accomplished using a 1-D ^{1}H NMR, 2-D homonuclear COSY, and 2-D NOESY NMR methods. Fortunately for compound **1**, this process is simplified highly due to the unusual nature of its 1-D ^{1}H NMR spectrum. A large body of spectral data previously reported[1] for precursor molecule [5-(8′-[4″-(8‴-[2‴′,5‴-dimethoxyphenyl]-1‴-naphthyl)-1″-phenyl]-1′-naphthyl)-10,20-diphenylporphinato]zinc(II) (**2**) made facile spectral assignments in **1**. Comparison of 1-D ^{1}H NMR spectral data obtained for **1** (Figure 1) and **2**[1] shows that the spectrum changes little upon transformation of dimethoxybenzene unit (**2**) to a benzoquinonyl moiety in compound **1**. The COSY data (Supporting Information) of compound **2** enabled straightforward assignment of both the Naphthalene I pillar (H_{11}−H_{16}) and the Naphthalene II pillar (H_5−H_{10}) protons (Figure 2).

The 1-D ^{1}H NMR spectrum of compound **1** manifests the characteristics previously enumerated for this class of π-stacked D-Sp-A compounds,[1] which include (i) distribution of aromatic resonances over a spectral window that spans 10.20−0.62 ppm, (ii) groupings of signals that derive from disparate shielding effects as a result of an upright, π-stacked geometry, and (iii) sharp resonances which exhibit little-to-no spectral overlap. Figure 1 divides the spectrum into two regions labeled A and B. Region A contains those resonances ascribed to the porphyrin β pyrrolic protons, the porphyrin 10,20-phenyl substituents, as well as the protons residing on the Naphthalene I pillar (Figure 2). Region B contains the resonances associated with the Naphthalene II pillar, the intervening phenyl spacer (H_1−H_4, Figure 2), and the protons residing on the quinonyl subunit.

(17) Brünger, A. T. *X-Plor Manual*; Yale University Press: New Haven, 1987; Version 3.1.
(18) Baysal, C.; Meirovitch, H. *J. Comput. Chem.* **1999**, *20*, 1659−1670.
(19) Allen, R., Doctoral Dissertation, University of Pennsylvania, 1999.
(20) Rees, P. B. *Acta Cystal. B* **1970**, *26*, 1311−1316.
(21) Molecular Simulations Inc.: San Diego, CA, 92121.

Porphyrinic Assignments. The distribution of the chemical shifts associated with the eight β pyrrolic doublets is characteristic of a 5-substituted 10,20-diphenylporphyrin.[22] Typically, this substitution pattern results in the observation of four sets of symmetry-related β protons; the magnitude of the chemical shift values for these nuclei decreases with increasing distance from the unsubstituted meso position. Using this chemical shift trend as a guideline, one would expect that the two protons flanking the unsubstituted meso position in **1** would resonate furthest downfield. This is indeed what is observed in the 1-D ^{1}H NMR spectrum of **1** (Figure 1). Unlike a 5-substituted 10,-20-diphenylporphyrin, which due to fast exchange of the pyrrolic N−H protons displays a spectral signature characteristic of C_{2v} symmetry, compound **1** exhibits eight unique β pyrrolic resonances and is thus pseudo-C_s symmetric. The observation of eight β pyrrolic resonances evinces that rotation around either the C_{meso}-to-$C_{1-naphthyl}$ and/or the $C_{8-naphthyl}$-to-$C_{1-quinonyl}$ linkages are slow on the NMR time scale, since either of these two dynamic processes would generate a plane of symmetry bisecting the porphyrin 5- and 15-meso carbon atoms, resulting in the observation of 4 sets of porphyrin β-pyrollic doublets. The H_{21}, H_{22} atoms (Figure 2) exhibit the furthest downfield chemical shift (9.28 and 9.36 ppm, respectively) of the eight β protons. A clear set of NOESY-derived cross-peaks correlating the β pyrrolic protons H_{21} and H_{22} with the meso proton (H_{20}) corroborates this assignment. Having firmly established the identity of the downfield β protons as the H_{21}/H_{22} set, the assignment of their *J*-coupled partners (H_{24} δ = 8.99 ppm, H_{23} δ = 8.88 ppm) was straightforward with the aid of a COSY spectrum (Supporting Information).

The NOE assignments of the remaining 4 β pyrrolic protons ($H_{25}-H_{28}$, Figure 2) is critically important in the solution structural determination of compound **1**. The spatial proximity of these nuclei with respect to the H_1 and H_2 protons residing on the intervening phenyl spacer provides key quantitative information regarding the geometrical relationship between the phenylene spacer and the porphyrin macrocycle. As shown in Figure 1, there exist three doublets in the region of 8.71−8.58 ppm; on the basis of the chemical shift pattern typical of 5-substituted-10,20-diphenylporphyrins,[22] two of these doublets must correspond to the H_{25} and H_{26} nuclei. This assumption was verified by NOESY spectral data which show distinctive cross-peaks that correlated the H_{25} and H_{26} β pyrrolic nuclei with the four ortho protons of the 10,20-diphenylporphyrinic substituents (vide infra).

The observation of 4 nonequivalent ortho resonances for the 10,20-diphenylporphyrinic substituents derives from two factors: (i) hindered rotation of the naphthalene-pillared porphyrin superstructure about the C_{meso}-to-$C_{1-naphthyl}$ bond (Figure 2) and (ii) the fact that Naphthalene I−phenylene−Naphthalene II−quinone unit is asymmetric. These structural constraints discriminate an α and β face of the porphyrin macrocycle (Figure 3) and define a unique magnetic environment for the 10-and 20-phenyl ortho protons. The substantial broadening of the four 10- and 20-phenyl ortho proton resonances is consistent with the established low-frequency librations and the modest rotational barrier for the 10- and 20-phenyl substituents about the their respective $C_{1'}-C_{meso}$ bonds.[23−25]

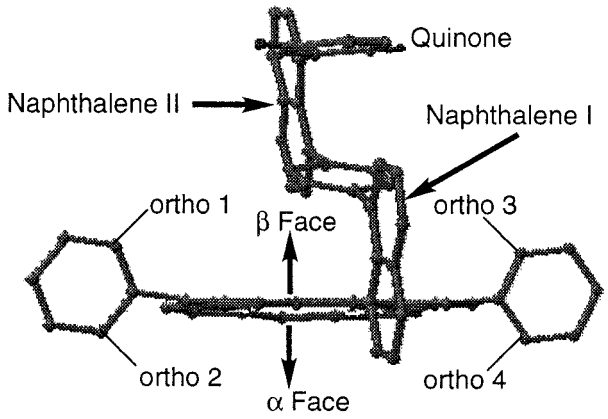

Figure 3. Ball and stick representation of compound **1.** An α and β face of the porphyrin macrocycle are discriminated due to the slow rotation of the (Naphthalene I)−phenyl−(Naphthalene II)−quinonyl structure about the C_{meso}-to-$C_{1'-Naphthyl}$ linkage. Four unique ortho resonances (labeled ortho 1−4) are observed in the ^{1}H NMR spectrum (Figure 1) of compound **1**.

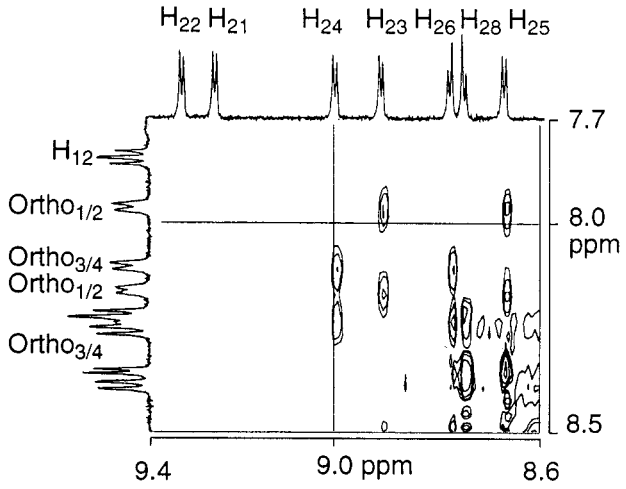

Figure 4. Expansion of the NOESY spectrum in the (7.7−8.5) × (8.6−9.4) ppm spectral domain. Experimental conditions: solvent = $CDCl_3$, temperature = 25 °C, τ_m = 800 ms. The NOESY cross-peaks correlate the H_{25}/H_{26} and H_{23}/H_{24} pyrrolic H-atom sets with the ortho protons of the porphyrin's 10,20-diphenyl substituents.

Figure 4 shows the NOESY cross-peaks correlating both the H_{25}/H_{26} and H_{23}/H_{24} pyrrolic H-atom sets with the ortho protons of the 10- and 20-phenyl groups. Noticeably, the doublet centered at 8.67 ppm is assigned to H_{28}. This assignment was supported by the NOESY data and deviates from the standard chemical shift profile of a 5-substituted-10,20-diphenylporphyrin. The NOESY spectra also aided in the assignment of the protons H_{25} and H_{26}.

Differentiating the H_{25} and H_{26} nuclei, as well as the H_{27} nucleus from the H_{28} β-pyrrolic proton, requires analysis of additional NOE data. The fact that the porphyryl, naphthyl, intervening phenyl, and quinonyl moieties of compound **1** possess severely restricted rotational degrees of freedom simplifies this task. For example, fast rotation of the quinonyl and/or intervening phenyl rings on the NMR chemical shift time scale would result in an averaging of the H_3 and H_4 resonances as well as the H_1 and H_2 signals. Instead, at ambient temperature (as well as at temperatures near 100 °C, vide infra) four unique

(22) DiMagno, S. G.; Lin, V. S. Y.; Therien, M. J. *J. Org. Chem.* **1993**, *58*, 5983−5993.

(23) Eaton, S. S.; Eaton, G. R. *J. Am. Chem. Soc.* **1975**, *97*, 3660−3666.

(24) Eaton, S. S.; Eaton, G. R. *J. Am. Chem. Soc.* **1977**, *99*, 6594−6599.

(25) Noss, L.; Lidell, P. A.; Moore, A. L.; Moore, T. A.; Gust, D. *J. Phys. Chem. B* **1997**, *101*, 458−465.

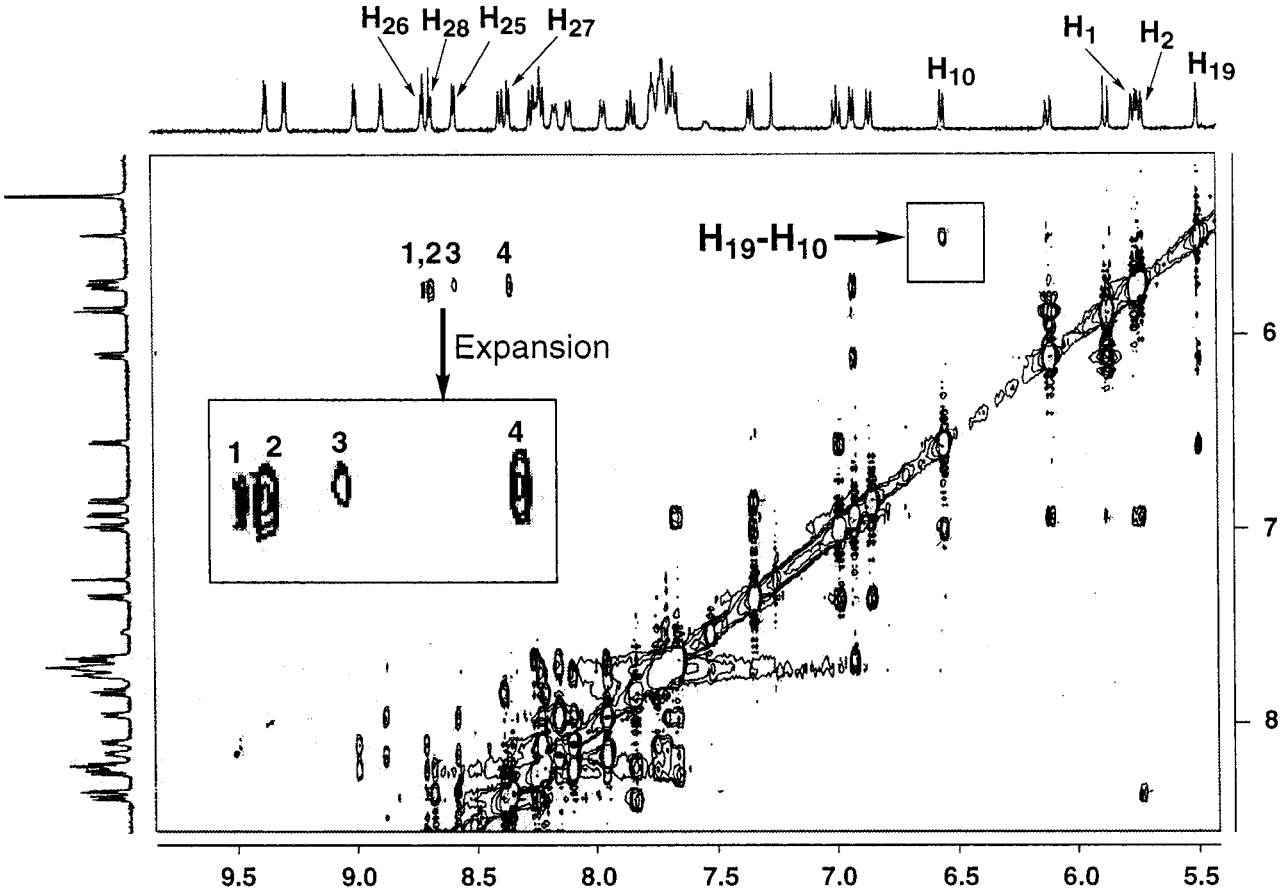

Figure 5. Expansion of the NOESY spectrum in the (5.1−8.6) × (5.4−9.9) ppm spectral domain. Experimental conditions: solvent = $CDCl_3$, temperature = 25 °C, τ_m = 800 ms. The labeled cross-peaks correlations are (1) $H_{26}-H_1$, (2) $H_{28}-H_1$, (3) $H_{25}-H_2$, and (4) $H_{27}-H_2$.

doublets corresponding to the H_{1-4} nuclei are observed in the ^1H NMR spectrum (Figure 1) in the region between 4.0 and 5.8 ppm.

NOESY Assignments Which Correlate Porphyryl, Phenyl, and Quinonyl Subunits. Because the three vinyl protons of the quinonyl moiety exhibit distinctive *J*-coupling patterns, it is possible to obtain unambiguous assignments for protons $H_{17}-H_{19}$. In particular, H_{19} centered at 5.49 ppm (Figure 1) displays a distinctive coupling with H_{17} (J = 2.5 Hz). The hindered rotation of the quinone ring about the $C_{8'''-naphthyl}$-to-$C_{1''''-quinonyl}$ linkage at room temperature causes the phenyl H_3, H_4, H_1, H_2 nuclei to reside in unique magnetic environments. This fact, coupled with the sub van der Waals interplanar separations manifest in 1,8-diarylnaphthalenic compounds, creates a situation in which H_{19} can only be juxtaposed to either H_4 or H_3.

The NOESY data correlate the doublet at 5.49 ppm (H_{19}) and the doublet centered at 4.23 ppm (J = 8.8 Hz), now designated H_4. With this assignment made, the H_4 resonance was then correlated with its *J*-coupled partner H_2 (δ = 5.73 ppm). Despite the existence of spectral overlap for H_1 and H_2 resonances in the 1-D ^1H NMR spectrum (Figure 1), corresponding cross-peaks in the NOESY experiment are not overlapping (Figure 5). Note that a simple molecular mechanics-based structural model for **1** would predict that protons H_1 and H_2 reside on the periphery of the porphyrin's shielding region, while the H_3 and H_4 nuclei are fixed directly in the shielding region; the H_3 and H_4 resonances would thus be expected to lie further upfield than their respective *J*-coupled partners (H_1 and H_2), supporting the NOESY data that place the mean chemical shift of H_1 and H_2 downfield from that of H_3 and H_4 by approximately 1.6 ppm. The evaluation of NOESY cross-peak correlations allows differentiation of H_4 and H_3, and thus unique identification of the $H_{25}-H_{28}$ β pyrrolic nuclei.

The NOESY spectrum displayed in Figure 5 shows the 4 cross-peaks arising from the close interspatial separation of the β pyrrolic $H_{25}-H_{28}$ nuclei with the intervening phenyl spacer protons H_1 and H_2. Cross-peaks labeled 2 and 4 (Figure 5) clearly display a more intense NOE than the cross-peaks labeled 1 and 3 (Figure 5). Using the X-ray crystallographic data available for 1,8-diphenylnaphthalene (Cambridge Database) as a guideline,[14−16] it is predicted that the internuclear distance separating H_2 from H_{27} should be approximately 1.2 Å smaller than the H_2-H_{25} separation, due to the outward splaying of the 1,8-naphthalene substituents. Cross-peaks 2 and 4, then, correspond to the NOEs between H_1-H_{28} and H_2-H_{27}, respectively rather than the more distant H_1-H_{26} and H_2-H_{25} interactions. From these data, it is possible to assign the β proton resonances $H_{25}-H_{28}$ (Figures 1 and 2).

Assignments Based on *J* Couplings. The wealth of detailed *J*-coupling information accessible in compound **1** enables differentiation of resonances assignable to porphyryl and naphthyl subunits. Scalar coupling constants for the porphyrin's β pyrrolic doublets (^3J = 4.5−4.7 Hz)[1] are significantly smaller than those manifest for any pair of naphthalenic protons ($^3J \sim$ 7.8 Hz),[1] and thus provide an important assignment criterion in the two narrow spectral regions where multiple signals appear. For example, in Figure 1 Region A, naphthyl and porphyryl protons H_{11}, H_{14}, and H_{27} resonate within a ~0.2 ppm window. Differentiation of the porphyrin β pyrrolic signal H_{27} from the two flanking naphthalenic signals is simplified due to its distinctive 4.7 Hz coupling with H_{25}. Similarly, in the upfield region spanning 6.2−5.4 ppm, signals from the spacer phenyl

Table 1. Comparison of Experimental Interproton Separations Determined from NOESY Spectral Data Obtained for Compound **1** with the Analogous Distances of $\mathbf{1}_{low}$ Derived from the MD/SA Analysis

entry	H−H Label[a]	exptl dist (Å)	calcd dist for $\mathbf{1}_{low}$ (Å)[b]
1	H_7-H_8[e]	2.37	2.34
2	H_1-H_{26}	4.00	4.12
3	H_1-H_{28}	2.98	3.21
4	H_2-H_{27}	3.16	3.22
5	H_2-H_{25}	4.87	4.05
6	$H_{16}-H_{17}$	3.09	2.40
7	H_5-H_3	2.93	3.26
8	H_5-H_4	3.28	3.64
9	H_6-H_{20}	3.86	3.32
10	$H_{10}-H_{19}$	3.27	3.31
11	$H_{19}-H_4$	3.06	2.92
12	$H_{16}-H_1$	*c*	3.51
13	$H_{16}-H_2$	*c*	3.42
14	H_5-NH	*d*	2.43

[a] See **Figure 2**. [b] $\mathbf{1}_{low}$ is one of 44 calculated structures sharing the lowest CHARMm energy of 77.5 kcal/mol. See text for details. [c] Data not included in the quantitative structural analysis because of $H_{16}-H_1$ and $H_{16}-H_2$ NOE cross-peaks overlap. [d] Data not included in the quantitative structural analysis. See text for details. [e] Taken as a known separation and used as a calibrant. See refs 14 and 15.

and quinonyl moieties resonate in close proximity. The three quinonyl protons H_{17-19} are distinguished from the phenylene protons H_{1-2} by their distinctive splitting pattern consisting of two doublets (H_{19}, $J = 2.5$ Hz; H_{18}, $J = 7.5$ Hz) and a doublet of doublets (H_{17}).

NOESY Data Correlating Orthogonal Aromatic Systems. The NOESY spectrum is replete with additional cross-peaks that correspond to magnetic interactions between nuclei residing on distinct aromatic components of compound **1**. For example, due to the coplanar arrangement of naphthalenic 1,8-substituents, H_{19} would be expected to reside within the allowable NOE contact range of H_{10}; such a cross-peak is indeed apparent in Figure 5. This intersubunit dipolar coupling between H_{19} and H_{10} helps to define the dihedral angle between the quinonyl and Naphthalene II pillar least-squares planes (vide infra). The well-resolved NOESY spectrum allows us to calculate all the distances between hydrogen atoms bound to orthogonal naphthyl, aryl, and porphyryl moieties. In the following calculations, these distances fix the remaining structural degrees of freedom for **1**, and highlight the unusual constraints provided by the 1,8-diarylnaphthyl structural motif.

A summary of all the intersubunit NOE data is included in Table 1. Entry 6 in Table 1, for example, defines the distance between H_{16} and H_{17} and aids in the computation of the geometrical relationship of the quinone with respect to the Naphthalene I pillar. Likewise, entries 7 and 8 help fix the dihedral angle between the phenyl spacer and Naphthalene II pillar; notably, because these experimentally determined H_5-H_4 and H_5-H_3 distances are both under 3.3 Å, it is clear that the range of dynamical motion for Naphthalene II pillar relative to the phenylene spacer is highly restricted. Entry 9 further delineates the geometrical relationship between the Naphthalene II pillar and the porphyrin macrocycle, limiting the magnitude of the dihedral angle between the naphthyl and porphyryl moieties. Entries 12−14 in Table 1 correspond to observed NOE signatures that are significant structurally, but were not included in the quantitative analysis of the 2-D NMR data. Spectral overlap in the NOE cross-peaks made accurate integration of the associated NOE volumes for entries 12 and 13 difficult. For the case of entry 14, the observed NOE corresponds to a dipolar interaction between H_5 and an internal porphyrinic N−H proton; although this result is qualitatively significant, and should be considered in any assessment of the geometry of the Naphthalene II pillar relative to the porphyrin central core, pyrrolic N−H tautomerism makes any NOE volume integration unreliable.

Computational Studies of Solution Structure. (a) General Approach. A set of 11 interproton distances which define key structural relationships in **1** were extracted from the NOESY spectrum (Table 1); these NOESY-derived constraints were used as restraining functions in the MD/SA calculations for compound **1**. The 50 lowest energy structures generated using the MD/SA analysis were further refined using CHARMm-based energy minimization; these studies determined the distribution of energies among the conformers and evaluated the extent to which the calculated structures were consistent with the empirical NOESY data.

(b) Initial Structural Considerations. The solution structure determined for compound **1** using ab initio simulated annealing computations that employed NOESY-derived distance constraints contrasts the majority of small molecule NMR structural determinations[26−29] that attempt to assign minimum energy structures to organic molecules that possess significant flexibility and considerable conformational mobility. Compound **1** belongs to a class of small-to-medium-size organic molecules lacking extensive dynamical degrees of freedom; this suggests that the collection of computed minimum energy structures for this species may display an unusual degree of conformational homogeneity. Moreover, because structural rigidity restricts available modes of conformational freedom in compound **1**,[26,29,30] the selection of a reasonable initial structure in these computations is assured.

(c) Force Field Development for Restrained MD/SA Analysis. The absence of a suitable parameter set for compound **1** in X-PLOR resulted in the independent development of both parameter and structure files. To this end, the significant body of relevant X-ray crystallographic data[14−16] available for 1,8-diarylnaphthalenes was used to build a force field to calculate the conformation of naphthyl, phenylene, and quinonyl superstructure. The porphyryl unit of **1** was parametrized based on X-ray crystallographic data obtained from a 5-aryl-10,20-diphenylporphyrin compound (See Experimental Section)**.** The structures of the ring systems in **1** are not expected to differ dramatically from those elucidated for the corresponding isolated aryl, porphyryl, and quinonyl species due to the planar aromatic nature of each of these modular components.

Because the initial ab initio SA calculations at high temperature ensure an adequate conformational search for all possible conformers of compound **1**, our general computational protocol utilizes the 50 structures generated from the ab initio SA calculations as *highly refined* initial structures for the CHARMm restrained molecular mechanics minimizations. It is worth noting that the choice of bond, angle, dihedral angle, and improper angle force constant data proves less crucial in NMR structural determination calculations compared with standard molecular mechanics calculations.[17] In this context, two main factors must be considered when compiling force constant data for compound **1**. First, the high temperatures associated with the ab initio SA

(26) Nevins, N.; Cicero, D.; Snyder, J. P. *J. Org. Chem.* **1999**, *64*, 3979−3986.
(27) Kozerski, L.; Kawecki, R.; Krajewski, P.; Gluzinski, P.; Pupek, K.; Hansen, P. E.; Williamson, M. P. *J. Org. Chem.* **1995**, *60*, 3533−3538.
(28) Paloma, L. G.; Guy, R. K.; Wrasidlo, W.; Nicolaou, K. C. *Chem. Biol.* **1994**, *1*, 107−112.
(29) Reggelin, M.; Hoffmann, H.; Kock, M.; Mierke, D. F. *J. Am. Chem. Soc.* **1992**, *114*, 3272−3277.
(30) Neuhaus, D.; Williamson, M. *The Nuclear Overhauser Effect In Structural And Conformational Analysis*; VCH Publishers: New York, 1989.

Table 2. Distribution of Low-Energy Structures for Compound **1** Determined from ab Initio SA Calculations and the CHARMm-Restrained Minimizations

	initial ab initio SA (X-Plor)[a]		final CHARMm restrained minimization[b]
	constraints included[c]	no constraints included	constraints included[c]
structures with NOE violations >0.5 Å	0		2
structures with NOE violations >0.2 Å	9		4
root-mean-square deviations	0.51 Å[d]	2.40 Å[d]	<0.10 Å[e]
energetic distribution of the lowest energy conformations	42 structures within 9 kcal/mol of $\mathbf{1}_{low}$		44 structures within 1 kcal/mol of $\mathbf{1}_{low}$[f]

[a] See refs 3−6 and 18. [b] See Experimental Section and ref 21. [c] Calculations included 11 distance constraints derived from quantification of NOESY cross-peak data listed in Table 1 (entries 1−11). [d] An average structure was calculated based on 50 conformers from the hybrid MD/SA analysis which considered the entire 52 carbon atom framework of **1**. The RMSD value of the 50 conformers is relative to this average structure. [e] The root-mean-square deviation calculation considered the entire 52 carbon framework of all 50 conformers and is relative to the lowest energy conformer, $\mathbf{1}_{low}$. [f] See Figure 6.

simulations require a significant scaling of all force constants to retain structural integrity and reasonable degrees of porphyryl, phenyl, and naphthyl ring planarity. Second, because the ab initio SA analysis was being used as a conformational searching tool, with the structures calculated from this analysis further minimized using a well established and widely accepted force field, force constant data for the X-PLOR calculations need only be approximate.[17,31]

(d) Ab Initio SA Analysis. Due to the fact that 1-D and 2-D NMR evidence strongly suggests that **1** adopts an upright π-stacked arrangement in solution,[1] the choice of the basic templated structure geometry for the ab initio SA calculation[17] is not controversial. The calculation was performed with 6000 steps of molecular dynamics at 2000 K with a time step of 0.005 ps. The total number of cooling steps was 1000 to reach a final temperature of 100 K. Using a random seed generator built into the X-PLOR program, we generated 50 low-energy structures. These 50 structures were then subject to a MD/SA slow cooling refinement process in which van der Waals radii were described by a full Lennard-Jones potential.[17]

(e) Comparison of NOE Data with ab Initio SA Determined Structures. The 50 refined structures were evaluated for NOE violations in excess of 0.5 Å, which represents the limit of confidence for the NMR measurements (Table 2); all 50 structures satisfied this conformational restraint. Remarkably, when more stringent criteria were used (i.e., a 0.2 Å NOE violation limit), 41 of these 50 computed minimum energy structures were finally accepted (Table 2). These structures generated from the ab initio SA calculations demonstrate not only excellent accuracy in their computed interproton distances with respect to the experimentally measured distances, but also high precision. An average structure was calculated from the 50 refined conformers that considered **1**'s entire 52 carbon atom framework**.** The root-mean-square deviation of the 50 conformers with respect to the consensus structure was calculated to be 0.51 Å (Table 2).

The relative energies[32] of the 50 ab initio SA derived structures show that 42 of these refined structures reside within a tight 9 kcal/mol energy domain; 6 of the 8 remaining conformers have energies varying from 11 to 17 kcal/mol above the lowest energy structure. The final two conformers had energies exceeding the lowest energy structure by >29 kcal/mol. The fact that 42 of the calculated structures have an energetic spread of 9 kcal/mol compares well with studies by Bruice and co-workers[11,12] in which the solution structure of a capped porphyrin was determined by 2-D NMR in conjunction with distance geometry calculations. In these studies, after grouping the 100 calculated structures into 13 structural subclasses and looking at the lowest energy conformer in each grouping, it was found that the 13 conformers varied in CHARMm energy by approximately 10 kcal/mol.[11,12] Clearly, a notable aspect of the ab initio SA determined structures for compound **1** with respect to these studies is the fact that 42 of the 50 low-energy structures belong to a single structural subclass.

The 50 structures derived from the hybrid MD/SA calculations represent excellent starting conformations for the second phase of the structural calculations, CHARMm-based restrained molecular mechanics. First, the fact that 41 of the calculated structures show no NOE violations greater than 0.2 Å and all 50 structures show NOE agreement under 0.5 Å demonstrates that there is an excellent correlation between the calculated and experimentally determined structures. Second, the 50 calculated structures exhibit significant conformational homogeneity as expressed in a root-mean-square value of 0.51 Å for the entire 52 carbon skeleton. Third, the hybrid MD/SA analysis returned 42 of the 50 structures within a 9 kcal/mol energy distribution. While direct quantitative comparison with other small molecule solution structure determinations is difficult because the criteria used to evaluate the accuracy of calculated structures varies significantly,[33] the hybrid MD/SA analysis clearly reproduces the overall structural features of **1**'s solution structure, providing a highly constricted subset of conformations for use in the final restrained minimization procedure.

(f) Computation of Structures in the Absence of NOE Restraints. To assess the effect that inclusion of NOESY data has upon the conformational search of compound **1**, the ab initio SA analysis was repeated in the absence of distance restraints. This baseline computation provides critical information regarding the impact NOESY constraint data has on shaping the outcome of these structural calculations. Repeating the ab initio SA analysis without NOE constraints generates a set of 50 conformers that display a wider range of conformational diversity as compared with those structures calculated with the inclusion of restraints. The effect of the distance restraints is best assessed by comparing the root-mean-square values of the two data sets (Table 2), obtained with (root-mean-square deviation = 0.51 Å) and without (root-mean-square deviation

(31) Marques, H. M.; Brown, K. L. *Coordination Chemistry Reviews* **1999**, *190−192*, 127−153.

(32) The energies reported for the 50 conformers represent CHARMm point energies. These energies are derived by reparametrizing the 50 conformers obtained during the X-Plor hybrid MD/SA analysis with CHARMm parameters (Supporting Information) and simply calculating a CHARMm energy at constant structure. The relative energies of the 50 conformers offer insight into the energetic distribution of the conformeric set but are meaningless with respect to absolute energies.

(33) The evaluation parameters used in assessing the quality of calculated structures are typically defined as a function of the force field employed. Root-mean-square calculations are dependent on the atom set included in the calculation.

= 2.40 Å) restraints; these data show that the NOE restraints do in fact play a key role in improving the quality of the calculated structures.

Remarkably, the 50 conformations obtained in the absence of constraints can be grouped into two structural subclasses by visual inspection. One family of conformers (36 structures) loosely resembles the structures calculated when distance restraints were employed, but show comparatively large variation of the dihedral angles between the porphyrin least-squares plane and the planes defined by the Naphthalene I and II pillars (~30 to −30 ° and 10 to −10 °, respectively). Although the vast majority of these conformers are thus inconsistent with both the 1-D ^{1}H NMR chemical shift data for the Naphthalene II pillar and NOESY-determined internuclear separations involving the porphyrin macrocycle (see entries 2−5, Table 1), similarity in gross structural characteristics (stacking of porphyrin, phenylene, and quinonyl units) demonstrates the robustness of the naphthyl pillaring motif to enforce a stacked arrangement of its 1 and 8 substituents.

The second family of 14 conformers corresponds to an improbable group of structures that are totally inconsistent with any of the experimental data. These structures display severe tipping of the Naphthalene I−phenyl−quinone assembly back away from the porphyrin (discussed in more detail later) allowing the Naphthalene II pillar to rotate such that the quinonyl ring is oriented into the porphyrin core. This highly variable group of structures obtained in the absence of the NOESY constraints does, however, evince the efficiency of the hybrid MD/SA protocol at sampling large areas of conformational space, and generating structures that clearly do not reside within the same local energy minimum.

The results of the unrestrained ab initio SA calculations highlight a unique feature of electron-transfer system **1**. Even in the absence of distance constraints, one of the two families of compounds resemble the low-energy structures determined when NOESY data had been included. Of course, as clearly evident in the root-mean-square deviation values for the unrestrained and restrained data sets (2.40 vs 0.51 Å), the inclusion of distance restraints significantly refines the quality of the calculated structure, and increases its precision. These studies indicate that the NOESY data are essential for (i) defining the relative orientation of the porphyrin and phenyl spacer's least-squares planes, (ii) fixing Naphthalene II's orthogonality with respect to the macrocycle plane, and (iii) verifying that the extent of porphyrin-based distortions that serve to reduce macrocycle aromaticity, particularly at the pyrrolic units that flank the Naphthalene I pillar, is minimal.

CHARMm-Based Restrained Molecular Modeling of the ab Initio SA Starting Structures. The 50 energy-minimized conformers derived from ab initio SA calculations were used as initial structures for restrained minimization in CHARMm. The main advantages of this final refinement procedure are the reliable parametrization of **1** in the CHARMm force field and the convenience of evaluating the relative stabilities of minimized conformers in terms of CHARMm energies. The quality of the low-energy calculated structure can be assessed by comparison (Table 1) with the NOESY-determined internuclear separations. NOE violations of 0.5 Å were found in only 2 of the 50 structures; lowering the acceptance threshold for the NOE violations to 0.2 Å excluded only 4 of the 50 structures, an improvement from the 9 structures found to have violations in the ab initio SA analysis (Table 2). The CHARMm-minimized structures show excellent consistency with the experimentally determined NOESY data. As expected, the longer NOE-determined contact distances (e.g., entry 5, Table 1) show larger discrepancies between the experimental and calculated distances.

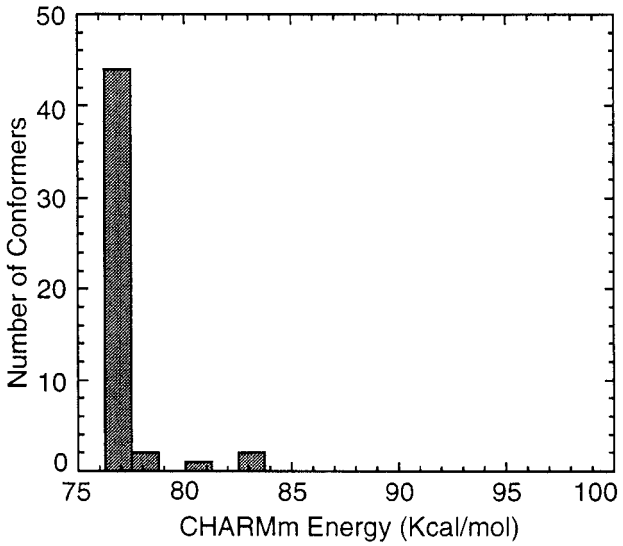

Figure 6. Histogram which shows the final CHARMm energetic distribution of the calculated structures. The calculated structures and their associated energies are the result of an initial conformational search using hybrid MD/SA followed by restrained minimization in the CHARMm force field.

A histogram showing the energetic spread of the 50 CHARMm-minimized structures is shown in Figure 6. The data show that 44 of the conformers are isoenergetic with a CHARMm energy of 77.5 kcal/mol; 5 conformers lie slightly higher in energy (<6 kcal/mol). One outlying conformer not included in Figure 6 has a CHARMm energy of 135 kcal/mol. The structural homogeneity of the 50 CHARMm-minimized conformers is rather remarkable. Comparing the lowest energy structure ($\mathbf{1}_{low}$) with the 49 structures represented on the Figure 6 histogram shows that the root-mean-square deviation is <0.1 Å.

Structural representations of $\mathbf{1}_{low}$ are shown in Figure 7 (van der Waals spheres at 80%). Several features of the calculated $\mathbf{1}_{low}$ structure deserve comment. A labeling schematic for the critical distances and angles used to characterize $\mathbf{1}_{low}$ is shown in Figure 8; the corresponding numerical data can be found in Table 3. One of the most striking features of the $\mathbf{1}_{low}$ structure is the closely packed, π-stacked arrangement of the porphyrin donor, intervening phenyl spacer, and the quinone acceptor. For example, the internuclear distance separating the C1 and C1′ carbon atoms (distance A, Figure 8B) of the 1-quinonyl and 1-phenyl substituents of Naphthalene II is 2.97 Å in $\mathbf{1}_{low}$, 0.4 Å below the van der Waals separation distance; these data are consistent with X-ray crystallographic data for the analogous distance separating the C1′ and C1″ carbon atoms in 1,8-diphenylnaphthalene (2.99 Å, Table 3; distance *A*, Figure 8A). Similarly, a sub van der Waals separation (2.97 Å) is also observed for the distance labeled *D* in Figure 8B. Note also that the *A* and *C* distances in $\mathbf{1}_{low}$ are consistent, suggesting that the hallmark sub van der Waals separation associated with simple 1,8-diarylnaphthalenes is maintained in **1** despite the incorporation of a large porphyrinic substituent at the Naphthalene I's 1-position.

Seminal work by both House[14] and Roberts[15] detailed the structural deformations which the naphthalene ring system undergoes to relieve considerable electrostatic repulsions between the compressed π-aromatic systems; note that the juxtaposed aromatic rings of 1,8-diphenyl naphthalene splay

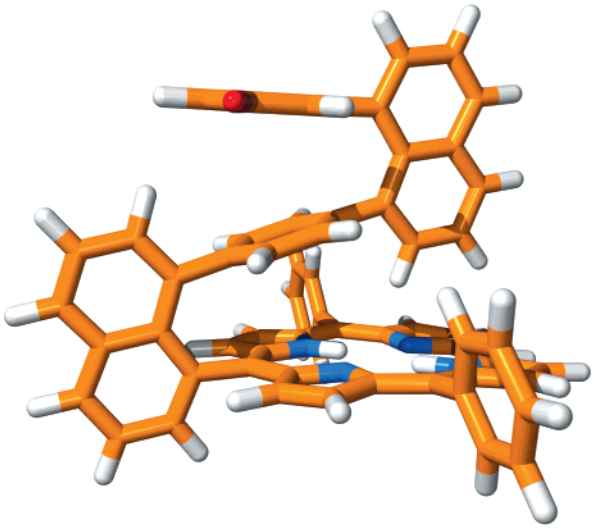

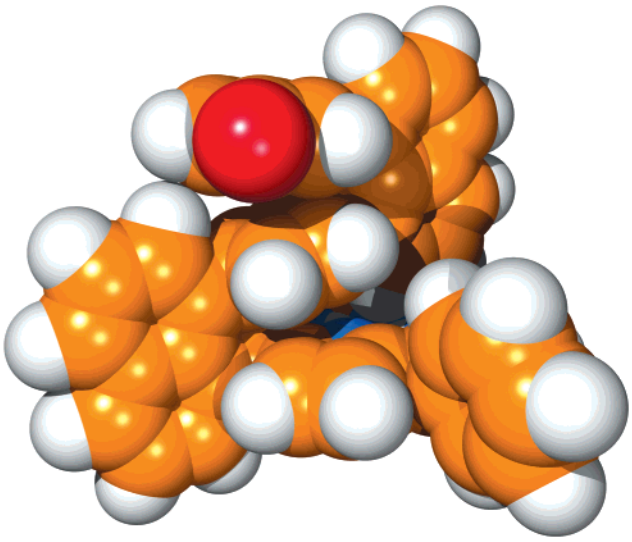

Figure 7. The structure of $\mathbf{1}_{low}$; van der Waals spheres are at 80%.

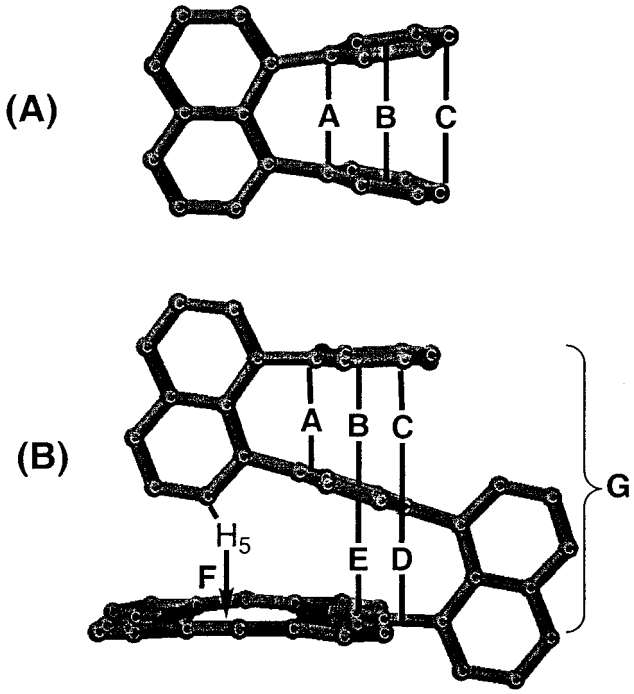

Figure 8. Schematic highlighting the key interplanar distances in (A) 1,8-diphenylnaphthalene and (B) compound **1**.

outward. The internuclear separation *A* (Figure 8A) in 1,8-diphenylnaphthalene is 2.99 Å, whereas distance *C*, which separates the 4′-phenyl−carbon centers, is 4.02 Å. The centroid−centroid distance *B* for 1,8-diphenylnaphthalene is intermediate between these two extremes at 3.53 Å; these metrical parameters correspond to an enlargement of the naphthalene C(1)−C(9)−C(8) angle by approximately 5° to a value of 126.2°.[14,15] Note that the analogous C(1)−C(9)−C(8) angles for Naphthalene I and Naphthalene II pillars are 128.0 and 127.4 °, respectively. Comparison of relevant metrical data in $\mathbf{1}_{low}$ shows a slightly attenuated degree of outward splaying relative to the 1,8-diphenylnaphthalene archetype, with a centroid-to-centroid distance *B* (Figure 8B) separating the quinone ring from the phenyl spacer of 3.46 Å, and a *C* distance of 3.95 Å. The vertical displacement of the centroid of the Naphthalene I pillar's 8′-phenyl substituent from the porphyrin least-squares plane (separation distance *E*, Figure 8B) is 3.35 Å, slightly lower than

Table 3. Comparative Distances Separating π-Stacked Ring Systems in Compound $\mathbf{1}_{low}$ (Determined from ab Initio SA Analysis Incorporating NOESY Restraints and Subsequent CHARMm Restrained Minimization) and 1,8-Diphenylnaphthalene[a]

	calcd distance (Å)	
label	$\mathbf{1}_{low}$[b]	1,8-diphenyl naphthalene[c]
A	2.97	2.99
B	3.46	3.53
C	3.95	4.02
D	2.97	
E	3.35	
F	2.17	
G	6.80	

[a] See Figure 8. [b] $\mathbf{1}_{low}$ is defined as the conformer with the lowest CHARMm energy of the 50 calculated structures. [c] Determined from X-ray crystallographic data. See refs 14 and 15.

the corresponding distance *B* separating the centroids of Naphthalene II's substituents (3.46 Å) and the phenyl-ring centroids of 1,8-diphenylnaphthalene (3.53 Å). Also included in Table 3 and highlighted in Figure 8B is separation *G*, which corresponds to the 6.80 Å vertical displacement of the quinone centroid from the porphyrin least-squares plane.

Perhaps the most remarkable aspect of the 1-D ^{1}H NMR spectrum of **1** is the chemical shift determined for aromatic proton H_5 (Figure 2), which resonates at 0.62 ppm (Figure 1, inset); note that the H_5 resonance is shifted *6.8 ppm upfield* from the analogous signal observed for 1-iodo-8-[4′-(8″-[2‴,5‴-dimethoxyphenyl]-1″-naphthyl)-1′-phenyl]naphthalene. Related NMR studies by Pascal and Van Engen[34] show that strained cyclophanes such as 2,6,15-trithia[3^{4,10}][7]metacyclophane, in which an apical methine hydrogen is forced into the center of an aromatic ring (H-to-arene centroid distance = 1.69 Å, determined from X-ray crystallographic data[34]), display an unusual resonance at −2.84 ppm, 4.90 ppm upfield of the analogous methine proton signal observed for the acyclic model compound. Similarly, related cyclophanic architectures have been built that feature exceptionally small hydrogen-to-aromatic ring distances; for example, Boekelheide has shown that a sub van der Waals proton−proton separation of 2.16 Å exists in [2,2]metaparacyclophane-1,9-diene.[35]

(34) Pascal, R. A.; Winans, C. G.; Van Engen, D. *J. Am. Chem. Soc.* **1989**, *111*, 3007−3010.
(35) Boekelheide, V.; Anderson, P. H.; Hylton, T. A. *J. Am. Chem. Soc.* **1974**, *96*, 1558−1564.

Insight regarding the origin of this large upfield shift for H_5 in compound **1** is gleaned from metrical analysis of $\mathbf{1_{low}}$. The distance separating the H_5 nucleus from the porphyrin least-squares plane in $\mathbf{1_{low}}$ (*F*, Figure 8B) is 2.17 Å. The upright orientation of the Naphthalene II pillar in **1** directs H_5 into the porphyrin core, where it is flanked on either side by the porphyryl 10 and 20 substituents. The sub van der Waals positioning of H_5 relative to the aromatic porphyrin ring is most easily visualized in the space-filling representation of Figure 7.

Nonquantitative NOESY Data Consistent with the Computed $\mathbf{1_{low}}$ Structure. In addition to the NMR data which support the validity of the calculated structure $\mathbf{1_{low}}$, there exists substantial nonquantitative NOESY data that solidify the structural conclusions derived from the analyses of the 1- and 2-D ^{1}H NMR spectral data. The observation of a NOE between the H_5 resonance (0.62 ppm) and the internal N−H signal (−3.35 ppm) is consistent with the positioning of the H_5 nucleus in the porphyrin central core. Likewise, NOESY cross-peaks observed from dipolar interactions involving H_6-H_{20}, H_6-H_{21}, and H_6-H_{22} support an NMR-time scale average upright structure for Naphthalene II. The mere observation of these medium-to-long-range NOEs involving the H_6 proton with *both* the H_{22} and H_{21} β pyrrolic protons are indicative of rigid conformation where the Naphthalene II pillar's average position is fixed upright and centered between the two porphyryl β proton resonances. These experimental results are clearly satisfied in the calculated structure $\mathbf{1_{low}}$ where the distances separating H_6-H_{22} (4.14 Å) and H_6-H_{21} (4.19 Å) are, within the limitations of this analysis, identical. To fully appreciate the structural significance of these results, it is worthwhile to consider the spectroscopic consequences that would be manifest in the NOESY spectrum if the Naphthalene II pillar could access a wide range of dihedral angles with respect to the porphyrin plane. Tilting motions of the Naphthalene II unit cause the H_9-H_{10} nuclei to approach either the H_{21} or H_{22} β pyrrolic protons. If, for example, the Naphthalene II moiety tilted toward the H_{22} nucleus, a significant increase in the distance separating the H_6 and H_{22} would result, reaching a maximum value (∼7 Å) when Naphthalene II achieves coplanarity with the porphyrin least-squares plane. If the compound **1** structure were not rigid, such large-amplitude tilting motions would cause the average H_6-H_{21}/H_{22} distance measured via NOESY to increase from the experimentally determined value of ∼4 Å toward the 7 Å limit. Even a marginal increase of the average NMR-time scale H_6-H_{21}/H_{22} distances would place the corresponding NOEs out of the experimentally measurable range (>5 Å).[30] Similarly, if the low-energy structures featured tilting of Naphthalene II toward either the porphyryl H_{21} or H_{22} nuclei, and the barrier to an upright Naphthalene II intermediate was large with respect to *kT*, an asymmetric NOE response for the H_6-H_{22} and H_6-H_{21} dipolar interaction would be observed, which was not the case. In sum, the experimental data can only be rationalized within the context of a structure in which the average position of the H_6 resonance lies equidistant between the H_{21} and H_{22} protons thereby exhibiting weak, yet measurable, NOESY cross-peaks between H_6 and the H_{21}/H_{22} nuclei.

Variable-Temperature ^{1}H NMR Spectroscopy. Because compound **1** features 38 fully aromatic resonances spread over a 9.6 ppm spectral window (Figure 1), 1-D NMR spectroscopy defines a simple method to probe temperature-dependent solution-phase dynamics. These studies complement the ab initio SA analysis and provide insight into the degree to which the π-stacked geometry of $\mathbf{1_{low}}$ remains robust with increasing temperature. The primary objectives of these variable-temperature (VT) ^{1}H NMR experiments are the delineation of the temperature-dependent conformational dynamics of Naphthalene I and II pillars and the elucidation of the magnitude of rotational barriers associated with the 1,8-diarylnaphthalene ring system.

Temperature-dependent ^{1}H NMR spectra of compound **1** in d_6-DMSO (Figures 9−11) were recorded over a 30−120 °C range. The spectral features observed in d_6-DMSO at 30 °C were very similar to those observed in $CDCl_3$; note that H_5's dramatic upfield chemical shift ($\delta = 0.62$ ppm, $CDCl_3$) remains evident ($\delta = 0.44$ ppm, d_6-DMSO, Figure 11). The H_1 and H_2 resonances which partially overlapped in the $CDCl_3$ spectrum are advantageously resolved ($\Delta\delta = 0.2$ ppm) in the d_6-DMSO spectrum (Figure 10). Heating the d_6-DMSO sample in 10 °C increments from 30 to 120 °C evinces (i) the absence of significant changes in either chemical shift or line shape for any of the Naphthalene I or Naphthalene II protons and (ii) rotation of the quinonyl ring at high temperatures. Fast rotation of the quinonyl ring about the $C_{8'''-\text{naphthyl}}$-to-$C_{1''''-\text{quinonyl}}$ bond gives rise to a pseudosymmetry plane bisecting the porphyrin 5- and 15-*meso* carbon atoms as well as the 1- and 4-positions of the intervening phenyl and quinonyl rings; the magnetic environments of protons residing on either side of the symmetry plane become increasingly similar with augmented temperature, causing symmetry-related pairs of resonances to eventually coalesce (see Figures 9 and 10). The affected resonances include the porphyrin β pyrrolic protons ($H_{21}-H_{28}$) (Figure 9) as well as the intervening phenyl protons (H_1-H_4) (Figure 10). As has been noted previously, these VT ^{1}H NMR spectra manifest the characteristic spectral signatures associated with the fast rotation of two 10- and 20-phenyl rings about the $C_{1'}-C_{meso}$ linkage (Figure 9).[23,24,36]

The proposed π-stacked solution structure of $\mathbf{1_{low}}$ positions the Naphthalene I and Naphthalene II pillars upright and orthogonal with respect to the porphyrin least-squares plane. Note that the spectra displayed in Figures 10 and 11 demonstrate that the naphthalenic resonances do not broaden or experience significant changes in chemical shift with increasing temperature. The VT ^{1}H NMR data thus show convincingly that Naphthalene I and II pillars experience only relatively small amplitude dynamical motions over the 30−120 °C temperature domain and maintain a perpendicular arrangement with respect to the porphyrin macrocycle even at high temperature. This is evinced quite clearly in Figure 11, which shows that the magnitude of the dramatic upfield shift experienced by Naphthalene II's H_5 nucleus, which derives from its sub van der Waals positioning in the porphyrin's shielding region, remains essentially unchanged throughout this series of spectra. Certainly, if the Naphthalene II unit experienced large-amplitude motions that reduced the porphyrin−naphthalene dihedral angle with increased temperature, one would expect to observe a substantial change in the average magnetic environment sampled by the H_5 nucleus. The unusual chemical shift and sharp signal for the H_5 resonance thus constitutes an important probe of local structure and the dihedral angle between the porphyrin and Naphthalene II least-squares planes. It is important to point out that the weak dependence of H_5's line shape and chemical shift upon temperature ($\Delta\delta = 0.25$ ppm, 30−120 °C) is mirrored by the H_6-H_{10} Naphthalene II protons as well as by the Naphthalene I $H_{11}-H_{16}$ nuclei.

While fast rotation of the quinonyl ring is the simplest explanation that accounts for the coalescence of the porphyryl

(36) Noss, L.; Liddell, P. A.; Moore, A. L.; Moore, T. A.; Gust, D. *J. Am. Chem. Soc.* **1997**, *101*, 4458−465.

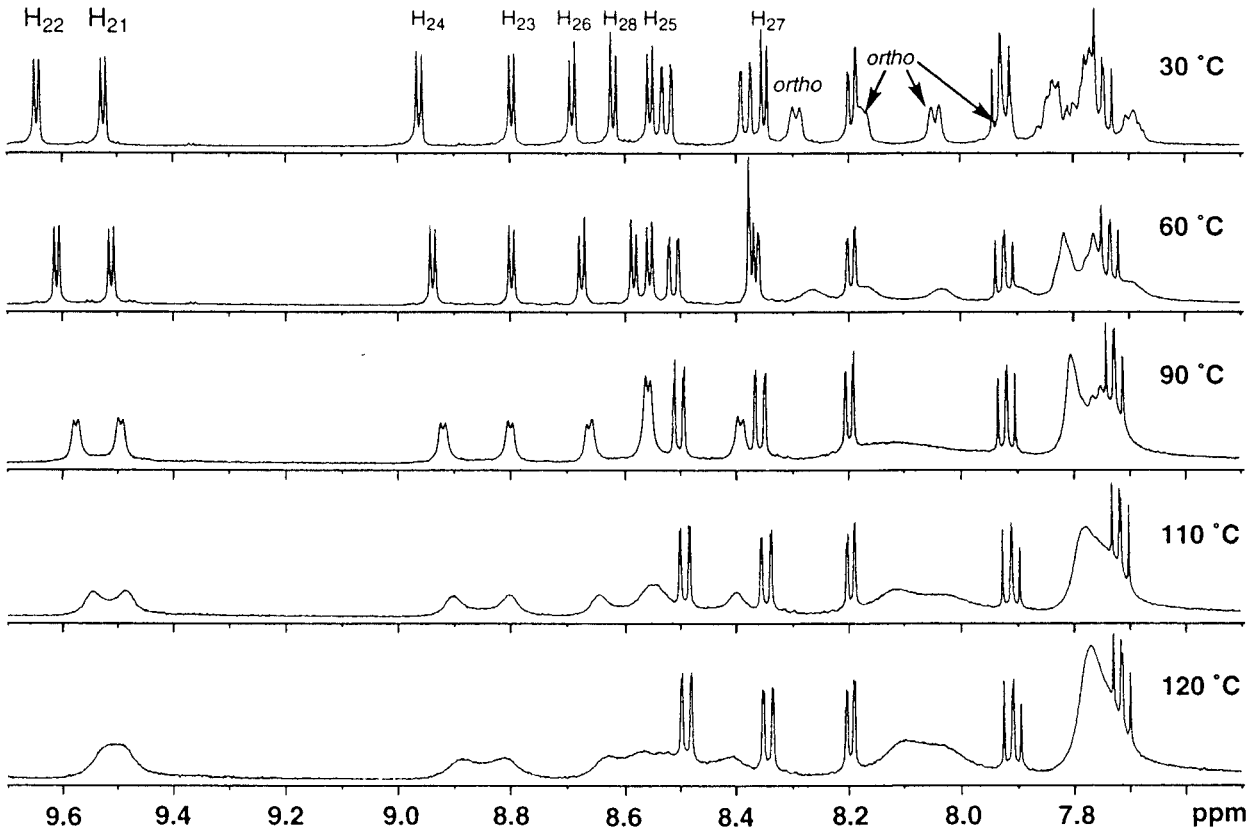

Figure 9. 500 MHz variable-temperature ^{1}H NMR spectrum of 5-[8′-(4″-[8‴-(2⁗,5⁗-benzoquinonyl)-1‴-naphthyl]-1″-phenyl)-1′-naphthyl]-10,20-diphenylporphyrin (**1**) in the 9.7−7.5 ppm region. Solvent = d_6-DMSO.

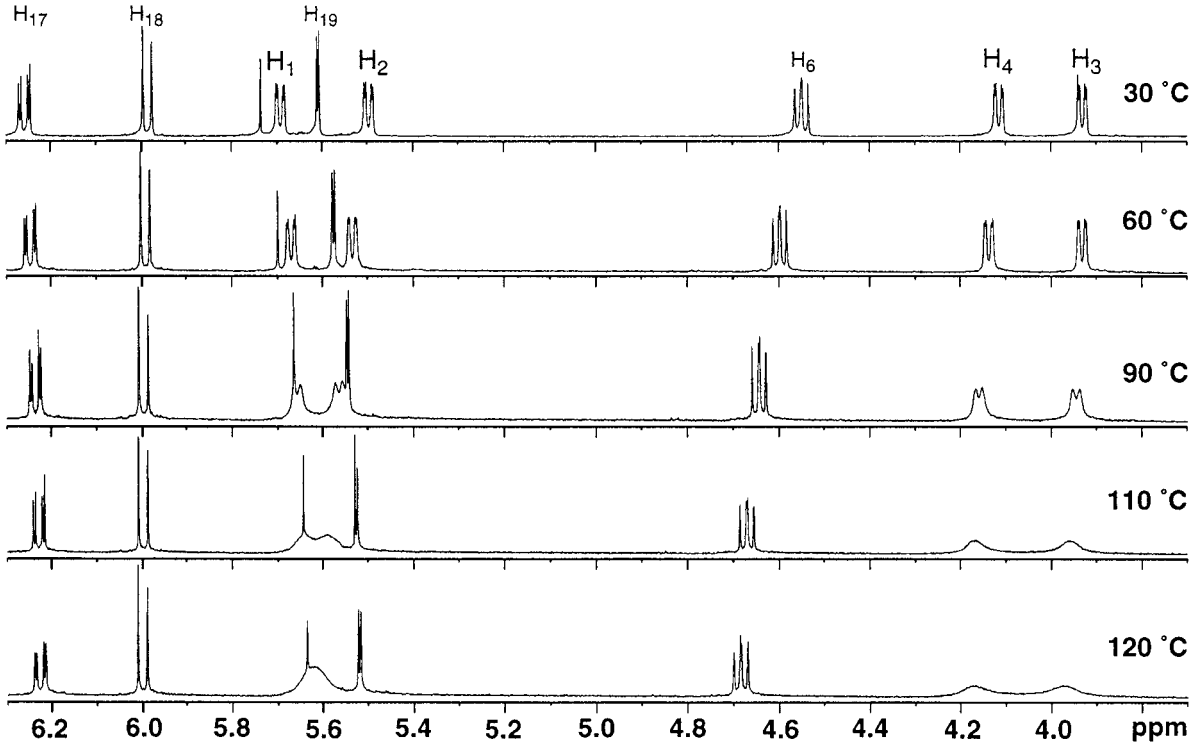

Figure 10. 500 MHz variable-temperature ^{1}H NMR spectrum of 5-[8′-(4″-[8‴-(2⁗,5⁗-benzoquinonyl)-1‴-naphthyl]-1″-phenyl)-1′-naphthyl]-10,20-diphenylporphyrin (**1**) in the 6.3−3.7 ppm region. Solvent = d_6-DMSO.

β and the intervening phenyl protons, a second ring rotation process involving the intervening phenyl moiety may also play a role in determining the temperature-dependent behavior of these resonances. In this regard, it is worth noting that parallel VT-NMR studies of [5-[8′-(2″,5″-dimethoxyphenyl)-1′-naphthyl]-10,20-diphenylporphinato]zinc(II) over an identical temperature domain show no evidence of dimethoxyaryl ring rotational dynamics.[1]

Selecting the $H_{22}-H_{21}$ β proton resonances, which are well-resolved at ambient temperature (Figure 9), and analyzing the

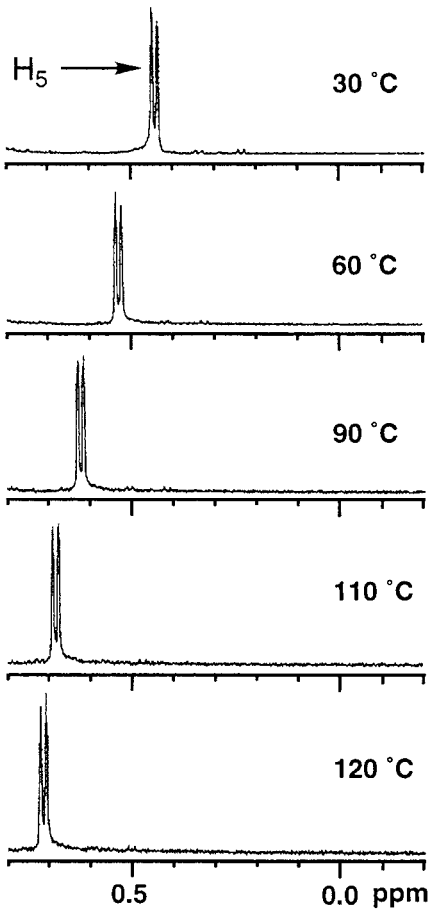

Figure 11. 500 MHz variable-temperature ^{1}H NMR spectrum of 5-[8′-(4″-[8‴-(2⁗, 5⁗-benzoquinonyl)-1‴-naphthyl]-1″-phenyl)-1′-naphthyl]-10,20-diphenylporphyrin (**1**) in the 0.8 to −0.2 ppm region highlighting the small change in H_5's chemical shift as a function of temperature. Solvent = d_6-DMSO.

VT behavior of these signals provides an estimate for the activation barrier for the quinonyl rotation of approximately 19 kcal/mol. Recalculating a rotational barrier using the coalescence temperature of the intervening phenyl protons H_1-H_2 (Figure 10) affords a similar value of 19 kcal/mol. The similarity of the magnitudes of these two rotational barriers suggests that the coalescence of the H_1-H_2 resonances results from the same dynamical process that causes coalescence in the $H_{22}-H_{21}$ β proton set.[1] Note that this calculated barrier to rotation is intermediate with respect to those determined for mono and bis-ortho-substituted 1,8-diarylnaphthalenes (1-phenyl-8-(*o*-tolyl)-naphthalene, 14.7 kcal/mol;[37] 1,8-di-*o*-tolylnaphthalene, 24.1 kcal/mol[15]).

Summary and Conclusions

A series of uniquely rigid, π-stacked ET assemblies have been defined in which the interplanar distances between D, bridge, and A aromatic units are less than the sums of their respective van der Waals radii. The 1-D ^{1}H NMR and 2-D NMR data of these compounds show that (i) the structures constrain nuclei to reside in unusual and diverse local magnetic environments and (ii) the close contacts afforded by a sub van der Waals interplanar separation of D, Sp, and A give rise to a comprehensive set of structurally significant NOE signatures that can be used as constraints in quantitative structural calculations. Examination of such data using ab initio SA analysis shows that compound **1** constitutes an unusual example of a "small organic molecule" for which these analytical tools unequivocally determine a single unique structure in solution.

Acknowledgment. M.J.T. is indebted to the United States Department of Energy (DE-FG02-94ER14494) for their generous financial support of this work and thanks the Alfred P. Sloan and Camille and Henry Dreyfus Foundations for research fellowships.

Supporting Information Available: COSY spectra and tabulated NMR data (compound **1**), X-Plor parameter and topology files, as well as CHARMm parameter files, are available (PDF). This material is available free of charge via the Internet at http://pubs.acs.org.

JA010023T

(37) Cozzi, F.; Cinquini, M.; Annunziata, R.; Dwyer, T.; Siegel, J. S. *J. Am. Chem. Soc.* **1992**, *114*, 5729−5733.